NASA TECHNICAL NOTE

NASA TN D-6262

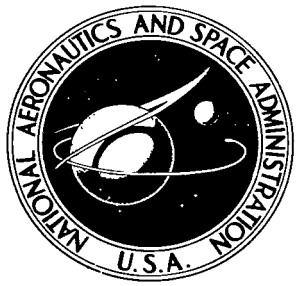

LINEARIZED THEORY OF STAGNATION REGION SKIN FRICTION AND MASS TRANSFER AT HYPERSONIC SPEEDS

by Kenneth K. Yoshikawa

Ames Research Center
Moffett Field, Calif. 94035

NATIONAL AERONAUTICS AND SPACE ADMINISTRATION • WASHINGTON, D. C. • MARCH 1971

1. Report No.	2. Government Accession No.	3. Recipient's Catalog No.
NASA TN D-6262		

4. Title and Subtitle	5. Report Date
LINEARIZED THEORY OF STAGNATION REGION SKIN FRICTION AND MASS TRANSFER AT HYPERSONIC SPEEDS	March 1971
	6. Performing Organization Code
7. Author(s)	8. Performing Organization Report No.
Kenneth K. Yoshikawa	A-3677
	10. Work Unit No.
9. Performing Organization Name and Address	129-01-02-05-00-21
NASA, Ames Research Center Moffett Field, Calif., 94035	11. Contract or Grant No.
	13. Type of Report and Period Covered
12. Sponsoring Agency Name and Address	Technical Note
National Aeronautics and Space Administration Washington, D. C. 20546	14. Sponsoring Agency Code

15. Supplementary Notes

16. Abstract

A linearized theory for stagnation region heat and mass transfer has been extended to include the shear stress. The method considers the momentum and energy equations which are uncoupled first and then linearized by the introduction of the effective values for the thermal and transport properties. Solutions of these equations are applicable at very high speeds, where conduction and shear stress in the shock layer and the interaction between the heated gas behind the shock wave and the injected or ablated gases must be considered. An explicit closed-form first-order solution has been obtained for the compressible, viscous shock-layer momentum equation with mass addition or suction.

Results of this analysis show that the effect of gas injection on shear gradient (skin friction) near the stagnation point strongly depends on the Stanton number without mass addition, wall temperature, relative injectant molecular weights, and the ratio of the averaged Peclet number between the free-stream and injected gases. The solution is substantiated by comparisons with exact solutions.

17. Key Words (Suggested by Author(s))	18. Distribution Statement
Compressible flow Laminar flow Aerodynamics Viscous shock layer with mass addition or suction Shearing stress reduction by gas injection Stagnation region flow Skin friction	Unclassified - Unlimited

19. Security Classif. (of this report)	20. Security Classif. (of this page)	21. No. of Pages	22. Price*
Unclassified	Unclassified	30	$3.00

*For sale by the National Technical Information Service, Springfield, Virginia 22151

SYMBOLS

a	parameter defined by equation (12)
B	blowing parameter, $\frac{\chi_w}{(St)_o}$ (eqs. (14))
$B_*, B_\dagger$	characteristic blowing parameter (eqs. (C9) and (C10))
c_p	specific heat with constant pressure
c_r	modification factor (eq. (A3))
erf	error function
H	free-stream total enthalpy, $h_\infty + \frac{1}{2} V_\infty^2$
h	enthalpy
$\overline{h}$	dimensionless enthalpy, $\frac{h}{H - h_w}$
j	total enthalpy, $h + \frac{1}{2}(u^2 + v^2)$
k	total thermal conductivity
k_a	constant defined in equations (7c)
k_w	effective ratio of mass-flow gradient (eq. (C7)), $\frac{(\chi_w')^{**}}{(\chi_w')^{*}}$
L	shock standoff distance
M	molecular weight of cold gas (at wall temperature)
$\overline{N}_f$	factor of proportionality defined in equation (15d)
Pr	Prandtl number
p	pressure
Q	function defined by equation (1) or (7c)
q	heat flux
R	body radius
Re	effective Reynolds number defined by equations (7c)

r	radial distance defined in figure 1
St	Stanton number, $\frac{q_c}{\rho_\infty V_\infty (H - h_w)}$
T	temperature
$\overline{T}$	$\frac{T}{T_s}$
U	value of u at the shock wave without heat conduction and shear stress, $V_\infty \frac{x}{R}$
u	x component of velocity
$\overline{u}$	$\frac{u}{U}$
V	velocity
v	y component of velocity
x	distance along body
y	distance normal to wall
β	Peclet number, $\frac{\rho_\infty V_\infty L}{(k/c_p)}$ (eqs. (7c))
γ	factor defined in equations (15c)
δ	boundary-layer thickness
$\delta^\dagger$	thermal boundary-layer thickness (eq. (B2))
$\delta_u^\dagger$	velocity boundary-layer thickness (eqs. (C4))
ε	density ratio across the shock wave, $\frac{\rho_\infty}{\rho_s}$
η	normalized distance from wall, $\frac{y}{L}$
λ	parameter defined in equations (15c)
μ	viscosity

ρ density

$\overline{\rho}$ $\dfrac{\rho}{\rho_{\text{(at sea level)}}}$

Φ shear reduction with gas injection, $\dfrac{\tau_w}{\tau_{wo}}$

ϕ shear reduction equivalent to $\psi\left[\lambda, \dfrac{B}{\sqrt{(Pr)_w}}\right]$ (eq. (15b))

ψ heat reduction with gas injection, $\dfrac{q_c}{q_{co}}$

χ dimensionless mass-flow parameter, $\dfrac{\rho v}{\rho_\infty V_\infty}$

χ_w' absolute value of $\dfrac{\partial \chi}{\partial \eta}$ near the wall

Subscripts

c convective at the surface

f foreign gases or equivalent foreign gas

m mixture

o no blowing

ref reference

s condition just behind shock wave

w wall

δ boundary-layer edge

∞ free-stream gas or conditions

Superscripts

* quantity for cold wall condition, $\dfrac{T_w}{T_s} \simeq 0$

** quantity for general wall condition, $\dfrac{T_w}{T_s} \neq 0$

' derivative

LINEARIZED THEORY OF STAGNATION REGION SKIN FRICTION AND MASS TRANSFER AT HYPERSONIC SPEEDS

Kenneth K. Yoshikawa

Ames Research Center

SUMMARY

A linearized theory for stagnation region heat and mass transfer has been extended to include the shear stress. The method considers the momentum and energy equations which are uncoupled first and then linearized by the introduction of the effective values for the thermal and transport properties. Solutions of these equations are applicable at very high speeds, where conduction and shear stress in the shock layer and the interaction between the heated gas behind the shock wave and the injected or ablated gases must be considered. An explicit closed-form first order solution has been obtained for the compressible, viscous shock-layer momentum equation with mass addition or suction.

Results of this analysis show that the effect of gas injection on shear gradient (skin friction) near the stagnation point strongly depends on the Stanton number without mass addition, wall temperature, relative injectant molecular weights, and the ratio of the averaged Peclet number between the free-stream and injected gases. The solution is substantiated by comparisons with exact solutions.

INTRODUCTION

Significant reductions in heat transfer and skin friction in the presence of foreign gas injection have been reported in a number of papers (refs. 1-7). These reductions are extremely important in the design of heat and shear resistant vehicles for very high speeds. Theoretical approaches to analyze the effect of mass addition on heat transfer and shear stress employ either (1) boundary-layer theory, or (2) shock-layer theory. The results may differ significantly, depending upon the flight conditions. For very high speed flight, shock-layer theory is essential for analyzing properly the problems of heat transfer and shear stress in the presence of mass addition.

Although the skin friction vanishes at the stagnation point of a blunt body, the ratio of shearing stress with mass addition to that without mass addition has a nonzero value. This ratio is important because it is related to the reduction in skin friction along the body surface, that is, the larger the reduction in gradient at the stagnation point, the smaller the skin-friction along the body surface.

The primary purpose of this report is, therefore, to find a simple solution, for the reduced shear, by extending the method of reference 1 to the shock-layer momentum equation. To find a solution the momentum equation is decoupled from the other conservation equations (continuity and energy equations) and linearized by means of an effective Reynolds number. A closed-form solution demonstrates the dependence of shear stress on the appropriate physical parameters. The method is substantiated by comparison with a number of numerical solutions of the exact equations.

ANALYSIS

A simplified momentum equation for the viscous, compressible flow in the neighborhood of a stagnation point has been considered. The reduction of the shear stress at the wall by transpiration or ablation gases emanating in hypervelocity flight will be emphasized. The present analysis considers the momentum and energy equations that will be decoupled by approximating the mass flow term in the equations. The equations are then linearized by the introduction of the effective values for the thermal and transport properties of the gases. To provide a physical insight into the parameters, a first-order solution is derived from the linearized equations for the case of no heat conduction and shear stress just behind the shock wave.

Finally, the primary effect of heat conduction and shear stress (postcooling effect) behind the shock wave on the flow parameters is determined by solving the linearized equations.

Although the shear stress at the stagnation point is zero, the ratio of shear stress with gas injection to that without gas injection is finite. In what follows, this ratio is designated by Φ and represents the reduction in shear gradient at the stagnation point. It may also be considered as a measure of the reduction of shear stress (skin friction) in the vicinity of the stagnation point.

Geometry and Assumptions

Figure 1 shows the geometry used in the analysis. The assumptions are as follows:

1. Steady axisymmetric stagnation-point flow
2. Thermodynamic equilibrium
3. No chemical reaction between free-stream and injection gases
4. Laminar continuum flow
5. Thin shock layer, $L/R \ll 1$
6. Small blowing rates, $\rho_w v_w/\rho_\infty V_\infty \ll 1$
7. Thermal diffusion and diffusion-thermal neglected

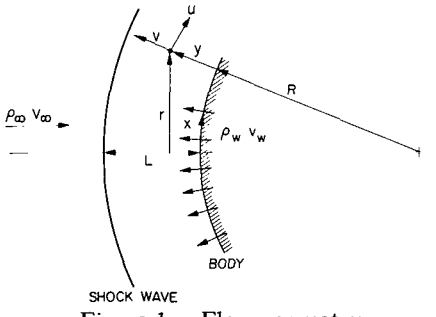

Figure 1.– Flow geometry.

Basic Equations and Boundary Conditions

The basic equations used for the present analysis are:

Continuity equation:

$$\frac{\partial}{\partial x}(\rho u r) + \frac{\partial}{\partial y}(Q \rho v r) = 0 \tag{1}$$

where

$$Q = 1 + \frac{y}{R}$$

Momentum equations:

$$\left.\begin{aligned} \rho u \frac{\partial u}{\partial x} + Q \rho v \frac{\partial u}{\partial y} &= -\left(\frac{\partial p}{\partial x}\right) + Q \frac{\partial}{\partial y}\left(\mu \frac{\partial u}{\partial y}\right) \\ \frac{\partial p}{\partial y} &= 0 \end{aligned}\right\} \tag{2}$$

Energy equation:

$$\rho u \frac{\partial j}{\partial x} + Q \rho v \frac{\partial j}{\partial y} = Q \frac{\partial}{\partial y}\left(k \frac{\partial T}{\partial y}\right) \tag{3}$$

Since the major portion of this study is concerned with the reduction of shearing stress in the vicinity of the stagnation point, the momentum and enery equations for the shock-layer flow are further simplified, for $\partial p/\partial x \simeq -\rho_s u_\delta (\partial u/\partial x)_\delta$, $\rho u(\partial j/\partial x) \ll \rho v(\partial j/\partial y)$, and $(1/2)(u^2 + v^2) \ll h$;

$$-Q \rho v \frac{\partial u}{\partial y} + Q \frac{\partial}{\partial y}\left(\mu \frac{\partial u}{\partial y}\right) = \rho u \frac{\partial u}{\partial x} - \rho_s u_\delta \left(\frac{\partial u}{\partial x}\right)_\delta \tag{4a}$$

$$\rho v \frac{\partial h}{\partial y} = \frac{\partial}{\partial y}\left(\frac{k}{c_p} \frac{\partial h}{\partial y}\right) \tag{4b}$$

The boundary conditions immediately behind the shock wave are altered by heat conduction and shear stress in the shock layer. The momentum and energy balances behind the shock wave may be written as

$$u_s = V_\infty \frac{x}{R} - \frac{1}{\rho_\infty V_\infty}\left(\mu \frac{\partial u}{\partial y}\right)_s \tag{5a}$$

$$h_s = H - \frac{1}{\rho_\infty V_\infty}\left(\frac{k}{c_p}\frac{\partial h}{\partial y}\right)_s \tag{5b}$$

where H is the free-stream total enthalpy.

Equations (4) are solved independently by the introduction of an equation for the normalized mass-flow distribution which is relatively independent of heat transfer. The mass-flow equation taken from reference 1 is

$$\chi \equiv \frac{\rho v}{\rho_\infty V_\infty} = \chi_w - \chi_w'\eta - (1 - \chi_w' + \chi_w)\eta^2 \tag{6}$$

where $\eta = y/L$ is the distance from the wall normalized by the shock-standoff distance, and χ_w' is the absolute value of $\partial\chi/\partial\eta$ near the stagnation point as shown in reference 1.

Transformed Equations

From equations (4) and (6), the dimensionless momentum and energy equations for the shock layer after some minor manipulation and approximation become (see appendix A)

$$\frac{d}{d\eta}\left(\frac{1}{Re}\frac{d\bar{u}}{d\eta}\right) - \chi\frac{d\bar{u}}{d\eta} = k_a \frac{L}{L_o} F(\eta) \tag{7a}$$

$$\frac{d}{d\eta}\left(\frac{1}{\beta}\frac{d\bar{h}}{d\eta}\right) - \chi\frac{d\bar{h}}{d\eta} = 0 \tag{7b}$$

where the dimensionless quantities are defined as

$$\left.\begin{aligned} \bar{u} &= \frac{u}{U} \simeq \frac{u}{V_\infty x/R} & F(\eta) &= \frac{[(\bar{u}_s\chi'/\chi_s')^2 - 2\varepsilon(1-\varepsilon)]}{Q} \\ \bar{h} &= \frac{h}{H - h_w} & Q &= 1 + k_a\varepsilon\frac{L}{L_o}\eta \\ Re &= \frac{\rho_\infty V_\infty L}{\mu}\ ; \quad \beta = \frac{\rho_\infty V_\infty L}{k/c_p} & k_a &\equiv \frac{1}{1 + \sqrt{(8/3)\varepsilon} - \varepsilon} \end{aligned}\right\} \tag{7c}$$

The physical quantities used in equations (7) are described in detail in appendixes A and C.

The boundary conditions taking the blowing from the wall into account and using the modified Rankine-Hugoniot condition across the shock wave are, from equations (5):

at $\eta = 0$

$$\left.\begin{aligned} \chi &= \chi_w \\ \bar{u} &= 0 \\ \bar{h} &= \bar{h}_w \end{aligned}\right\} \tag{8a}$$

at $\eta = 1$

$$\left.\begin{aligned} \chi &= -1 \\ \bar{u} &= \bar{u}_s = 1 - \left(\frac{1}{Re}\frac{d\bar{u}}{d\eta}\right)_s \\ \bar{h} &= \bar{h}_s = 1 + \bar{h}_w - \left(\frac{1}{\beta}\frac{d\bar{h}}{d\eta}\right)_s \end{aligned}\right\} \tag{8b}$$

Equations (7) are nonlinear second-order (ordinary) differential equations with nonlinear boundary conditions (eqs. (8)) and can only be solved numerically.

Linearized Solutions

Linearized solutions to the momentum and energy equations can be obtained explicitly when the Peclet number β and Reynolds number Re are replaced by values considered constant for the specified boundary temperature (see ref. 1 and appendix B); for example, for a cold wall ($\bar{T}_w \simeq 0$),

$$\left.\begin{aligned} \beta &= \beta^* \\ Re &= Re^* \end{aligned}\right\} \tag{9}$$

The linearized solutions become

$$\bar{u} = \bar{u}_c\left(c + k_a \int_o^\eta \left[\frac{1}{\bar{u}_c(\eta_1)}\right]^2 \left(\frac{L}{L_o} Re^*\right)\left\{\int_o^{\eta_1} \bar{u}_c(\eta_2) F(\eta_2) e^{[G(\eta_1)-G(\eta_2)]}\, d\eta_2\right\} d\eta_1\right) \tag{10a}$$

$$\bar{h} - \bar{h}_w = \left(\frac{d\bar{h}}{d\eta}\right)_w \int_o^\eta e^{(\beta^*/Re^*)G(\eta_1)}\, d\eta_1 \tag{10b}$$

where

$$\bar{u}_c(\eta) = \left(\frac{d\bar{u}_c}{d\eta}\right)_w \int_0^\eta e^{G(\eta_1)}\, d\eta_1 \tag{10c}$$

$$\left.\begin{aligned} c &= 1 - k_a \frac{L}{L_o} Re^* \int_0^1 \left[\frac{1}{\bar{u}_c(\eta_1)}\right]^2 \left[\int_0^{\eta_1} \bar{u}_c(\eta_2) F(\eta_2) e^{G(\eta_1)-G(\eta_2)}\, d\eta_2\right] d\eta_1 \\ \left(\frac{d\bar{u}_c}{d\eta}\right)_w &= \frac{1}{\left[\frac{1}{Re^*} e^{G(1)} + \int_0^1 e^{G(\eta_1)}\, d\eta_1\right]} \\ G(\eta) &= Re^* \int_0^\eta \chi\, d\eta_1 \end{aligned}\right\} \tag{10d}$$

Note that $\bar{u}_c$, the complementary solution to equation (7a), has the same form as equation (10b) with the constant β^* replaced by Re^*. For the general wall condition ($\bar{T}_w \neq 0$) the quantities marked by an asterisk in equations (10) will simply be replaced by double asterisks.

Since detailed analysis of the linearized solution to the energy equation and the heat reduction function ψ have been described in reference 1, only solutions to the momentum equation and the reduction in the shear gradient will be considered in the following sections.

First-Order Solution Without Postcooling

It is shown in reference 1 that for a large Peclet number ($\beta >> 1$) the boundary condition for the flow enthalpy given in equation (8b) is not affected by conduction behind the shock wave and $\bar{h}_s = 1 + \bar{h}_w$. Similarly, the boundary condition at the shock for the velocity in equation (8b) will not be significantly affected by conduction or shear stress for high Reynolds numbers ($Re >> 1$), and $\bar{u}_s \simeq 1$. It follows that one can derive a simple first-order solution for equation (10a) by taking only the leading term from the velocity distribution

$$\bar{u} \simeq c_1 \bar{u}_c + (1 - c_1)\eta + \ldots \tag{11a}$$

which satisfies boundary conditions $\bar{u}(0) = 0$ and $\bar{u}(1) = 1$ ($c_1 \simeq c$). Since the velocity gradient near the shock wave is relatively unchanged by mass addition (i.e., c is insensitive to blowing as shown by numerical solutions of eq. 10(d). See also ref. 3), the constant c_1 can be evaluated simply by integrating equation (7a) from $\eta = 0$ to $\eta = 1$ for $\chi_w = 0$. Thus,

$$\frac{1}{Re^*}\int_o^1 \bar{u}'\, d\eta - \int_o^1 \chi\bar{u}'\, d\eta = k_a \int_o^1 F(\eta)d\eta \qquad (11b)$$

Substituting equation (11a) into equation (11b) and using the relation

$$\int_o^1 \left(\frac{1}{Re^*}\,\bar{u}_c'' - \chi\bar{u}_c'\right)d\eta = 0$$

one can calculate the constant c_1 as

$$c_1 \simeq 1 - \frac{2k_a}{2 + \chi_w'}\left[1 - \left(\frac{\chi_w'}{\chi_s'}\right) + \left(\frac{\chi_w'}{\chi_s'}\right)^2 - 6\varepsilon(1 - \varepsilon)\right] \quad \text{for} \quad \varepsilon << 1 \ (Q \simeq 1) \qquad (11c)$$

Note that c_1 is independent of Re^*.

For $Re^* >> 1$ and $\chi_w << 1$, the complementary solution (eq. (10c)), will become (from ref. 1)

$$\bar{u}_c \simeq \frac{\bar{u}_s \operatorname{erf}\left[\sqrt{\frac{1}{2}(Re\chi_w')^*}\,\eta - a\right] + \bar{u}_s \operatorname{erf} a}{1 + \operatorname{erf} a} \qquad (11d)$$

The velocity gradient from equations (11a) and (11d) becomes

$$\left(\frac{d\bar{u}}{d\eta}\right)_w \simeq c_1 \sqrt{\frac{2}{\pi}(Re\chi_w')^*}\,\bar{u}_s\left[\frac{e^{-a^2}}{1 + \operatorname{erf} a}\right] + (1 - c_1) \qquad (12)$$

where

$$a = \left[\sqrt{\frac{1}{2}(Re/\chi_w')^*}\right]\chi_w$$

Equations for shear reduction- The reduction in shear gradient with mass addition can be obtained in terms of the blowing parameter B by dividing equation (12) by the same equation for $B = 0$. Thus, from equation (11a), the shear reduction can be written

$$\Phi \equiv \frac{\left(\frac{1}{Re}\frac{d\bar{u}}{d\eta}\right)_{w,B}}{\left(\frac{1}{Re}\frac{d\bar{u}}{d\eta}\right)_{w,B=0}} \simeq \left[\frac{c_1\left(\frac{1}{Re}\frac{d\bar{u}_c}{d\eta}\right)_{w,B} + \frac{1 - c_1}{Re_{w,B}}}{c_1\left(\frac{1}{Re}\frac{d\bar{u}_c}{d\eta}\right)_{w,B=0} + \frac{1 - c_1}{Re_{w,B=0}}}\right] \qquad (13a)$$

where the first term in the numerator and the denominator, which is a part of the complementary solution, can be derived by a method exactly analogous to the one used for the heat-transfer equation described in reference 1; that is,

$$\left(\frac{1}{Re}\frac{d\bar{u}_c}{d\eta}\right)_{w,B} \simeq \left(\frac{1}{Re}\frac{d\bar{u}_c}{d\eta}\right)^*_{w,B} \tag{13b}$$

The blowing parameter and effective Reynolds number (see appendix B) are given by

$$\left.\begin{aligned} B &= \chi_w/(St)_o \\ Re^* &= \beta^*/(Pr)_w \end{aligned}\right\} \tag{14}$$

where

$$(St)_o \simeq \sqrt{(2/\pi)(\chi_w'/\beta_o)^*}$$

Dividing equation (13a) by the first term in the numerator, and incorporating equations (12), (13b), (14) and appendixes C and D, one will obtain the following result:

$$\Phi = \left\{\frac{\phi\left[\lambda, \dfrac{B}{\sqrt{(Pr)_w}}\right] + \gamma \dfrac{(k/c_p)_w}{(k/c_p)^*}\dfrac{1}{L/L_o}}{1 + \gamma \dfrac{(k/c_p)_w}{(k/c_p)^*}}\right\} \tag{15a}$$

where

$$\phi\left[\lambda, \frac{B}{\sqrt{(Pr)_w}}\right] \simeq \left\{\begin{aligned} &\frac{1}{\sqrt{\frac{L}{L_o}\lambda^{B/B_\dagger}}}\left[\frac{e^{-\frac{1}{\pi}\frac{L}{L_o}\frac{\lambda^{B/B_\dagger}}{(Pr)_w}B^2}}{1 + \operatorname{erf}\sqrt{\frac{1}{\pi}\frac{L}{L_o}\frac{\lambda^{B/B_\dagger}}{(Pr)_w}}B}\right] && \text{for } B \le B_\dagger \\ &\frac{1}{\sqrt{\frac{L}{L_o}\lambda}}\left[\frac{e^{-\frac{1}{\pi}\frac{L}{L_o}\frac{\lambda}{(Pr)_w}B^2}}{1 + \operatorname{erf}\sqrt{\frac{1}{\pi}\frac{L}{L_o}\frac{\lambda}{(Pr)_w}}B}\right] && \text{for } B > B_\dagger \end{aligned}\right\} \tag{15b}$$

and

$$\left.\begin{aligned}
\gamma &= \frac{1}{2}\left(\frac{1 - c_1}{c_1}\right) \\
\lambda &= \sqrt{\frac{M_\infty}{M_f}}\,\overline{N}_f \\
B_\dagger &= \sqrt{(Pr)_w}\left[\frac{\pi}{(\chi_w')^*}\sqrt{\varepsilon\,\frac{M_f}{M_\infty}}\right] \\
\frac{L}{L_o} &= 1 + \sqrt{\frac{1}{\varepsilon}\left(\frac{M_\infty}{M_f}\right)}\,(St)_o B \\
(\chi_w')^* &= \frac{\sqrt{8\varepsilon(1 - \varepsilon)}}{1 + \sqrt{\frac{8}{3}\varepsilon} - \varepsilon}
\end{aligned}\right\} \qquad (15c)$$

In equations (15) $(Pr)_w$ is the Prandtl number evaluated at the wall condition. Note that the function ϕ (eq. (15b)) is identical to the heat-reduction function ψ, if the blowing parameter $B/\sqrt{(Pr)_w}$ is replaced by B. As shown in reference 1, the values of $\overline{N}_f$ given in equation (15c) are determined from either theoretical calculations or experimental data for the heat-transfer parameter by

$$\overline{N}_f \simeq \sqrt{\frac{M_f}{M_\infty}}\,\frac{\left(q_{co}\sqrt{\frac{R}{p_s}}\right)_\infty^2}{\left(q_{co}\sqrt{\frac{R}{p_s}}\right)_f^2} \qquad (15d)$$

For a first-order approximation, the factor $\overline{N}_f$ is found to be (for air as the main stream)

$\overline{N}_f \simeq \frac{5}{9}$ for monatomic gas

$\overline{N}_f \simeq 1$ for diatomic and some polyatomic gases[1]

Derivations of these values have been discussed in detail in reference 1.

[1] $\overline{N}_f \simeq 5/9$ for Freon gases (polymolecular), (data deduced from ref. 5).

Shear reduction for identical-gas injection- As a special case, equations (15) can be further simplified to

$$\Phi = \left[\frac{\phi(B) + \gamma \dfrac{(k/c_p)_w}{(k/c_p)^*} \dfrac{1}{L/L_o}}{1 + \gamma \dfrac{(k/c_p)_w}{(k/c_p)^*}} \right] \tag{16a}$$

where

$$\phi(B) = \frac{1}{\sqrt{\dfrac{L}{L_o}}} \left[\frac{e^{-\frac{1}{\pi} \frac{L}{L_o} \frac{1}{(Pr)_w} B^2}}{1 + \operatorname{erf} \sqrt{\frac{1}{\pi} \frac{L}{L_o} \frac{1}{(Pr)_w}}\, B} \right] \quad \text{for all } B \tag{16b}$$

It will be shown later that equations (15) and (16) are in satisfactory agreement with the numerical solutions of references 3 and 4.

When $L/L_o \simeq 1$, $\overline{T}_w \simeq 0$ and $\gamma \simeq 1$, equations (16a) may be expanded in a series to obtain

$$\Phi \simeq 1 - \frac{2}{\pi} \frac{1}{1 + \dfrac{(k/c_p)_w}{(k/c_p)^*}} \frac{B}{\sqrt{(Pr)_w}} + \ldots \tag{16c}$$

Effect of Heat Conduction and Shear Stress Behind the Shock Wave

The enthalpy and tangential velocity gradient immediately behind a shock wave (assuming the strong shock relation) will be altered significantly when heat conduction and shear stress become major factors in the energy and momentum balances within the shock layer. As in reference 1, this phenomenon is designated here as the "postcooling effect." When this phenomenon occurs, the first-order solution does not apply, and numerical solutions of the linearized equations (eqs. (10)) incorporating the effective Peclet number (or Reynolds number) from table 1[2] must be obtained. Preliminary effects of postcooling on the shear gradient reduction in the vicinity of the stagnation point will be discussed in the section "Results and Discussion."

[2]See appendix B.

RESULTS AND DISCUSSION

Calculations of the shear reduction at the stagnation point including foreign gas injection and suction are presented in this section for atmospheric flight conditions where the first-order solution applies. The postcooling effect on the shear stress at relatively low Reynolds numbers is also examined.

Results Without Postcooling

Shear reduction - identical gas injections- A comparison of the present first-order solution (eqs. (16a) and (16b) for p_s = 1 atm, T_s = 15,000° K, and R = 30 cm (1 ft) with the exact numerical solutions of Howe and Sheaffer[3] (ref. 3) is presented in figure 2 for identical gas injection. The present results show satisfactory agreement with the numerical solutions. Also presented is the solution obtained with the linear equation (16c), which is very close to the first-order solution for B < 1.

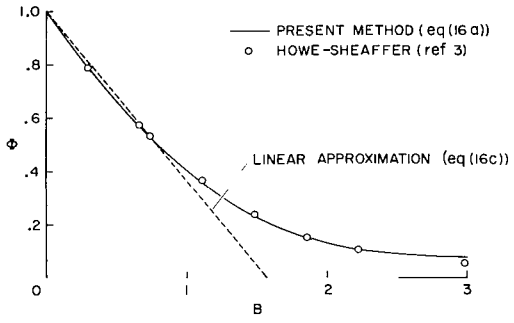

Figure 2.– Effect of gas injection on shear reduction – air injection (p_s = 1 atm, $T_s \simeq$ 15,000° K, and $T_w \simeq$ 1,000° K).

Effect of Stanton number- The present solutions show that the shear reduction function Φ, as for heat reduction (ref. 1), depends on the stagnation-point Stanton number $(St)_o$, which is a function of the product of free-stream density and body radius (ref. 1). As the stagnation-point Stanton number $(St)_o$ increases (i.e., the product of free-stream density and body radius decreases), the mass transfer becomes more effective in reducing the shear stress, as illustrated in Fig. 3. The present solutions and those of Howe and Sheaffer agree closely. A single correlation curve for the shock-layer theory can be obtained only if the Stanton number $(St)_o$ remains constant and $T_w/T_s \simeq 0$. The effect of the Stanton number (or $\rho_\infty R$) on shear stress (as well as heat transfer) is due essentially to the changes in the shock-layer thickness, which are accompanied by changes in the velocity gradient at the stagnation point. Experimental data on heat transfer and pressure changes due to the mass injection support the present conclusion (ref. 5).

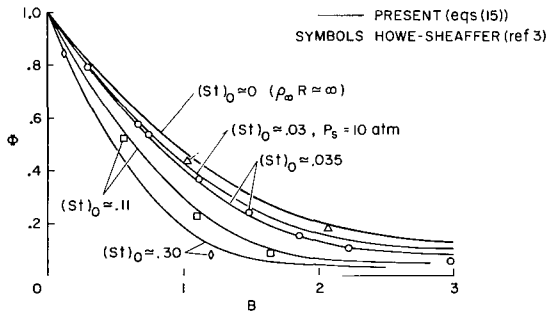

Figure 3.– Effect of Stanton number on shear reduction – air injection (p_s = 1 atm, $T_s \simeq$ 15,000° K, and $T_w \simeq$ 1,000° K).

[3]By courtesy of Howe and Sheaffer since numerical results for shear reduction were not presented in reference 3.

The effect of transport properties on shear reduction is also recognized; that is, (in fig. 3) the shear reduction curve for p_s = 10 atm and R = 3 cm (0.1 ft) is separated from that for p_s = 1 atm and R = 30 cm (1 ft) even though the Stanton number and wall temperature for both cases are about the same. This is due to the pressure dependence of the thermal and transport property parameter $(k/c_p)_w/(k/c_p)^*$. The heat-reduction function ψ, however, has a single correlation curve when the Stanton number is kept constant as demonstrated in reference 1.

Effect of wall temperature- In contrast to the heat reduction, the shear reduction is sensitive to the wall temperature. This dependency can be recognized immediately from the result of the first-order solution since the quantity $(k/c_p)_w$ in equation (15a) depends on wall temperature. The effect of wall temperature on shear reduction is shown in figure 4 for air injection. Generally, the higher the wall temperature, the less the shear reduction. The present methods are compared with the numerical calculation of reference 4, and the results show satisfactory agreement for a wide range of wall temperatures. To make this comparison, the parameter $\sqrt{1/\epsilon}\ (St)_o$, in equation (C8), is maintained at 0.15, the value used for the heat transfer case.

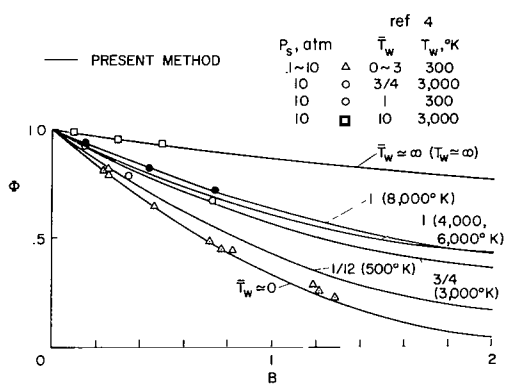

Figure 4.– Effect of wall temperature on shear reduction – air injection ($\sqrt{1/\epsilon}\ (St)_o \simeq 0.015$).

Shear reduction - foreign gas injection- Injecting gases different from the free-stream gas affects the shear reduction in the manner shown in figure 5. The present results, derived by means of equations (15), for p_s = 1 atm, T_s = 15,000° K, $\sqrt{1/\epsilon}\ (St)_o \simeq 0.15$, and for $T_w/T_s \simeq 0$, are compared with the boundary-layer solutions from reference 4. Satisfactory agreement is obtained over the entire blowing range including suction (B < 0). As can be recognized from equations (15), shear reduction for a cold wall ($T_w/T_s \simeq 0$) depends primarily on Prandtl number at the wall and on the blowing parameter B. The injection of light gases is more effective in reducing the rate of the shear stress near the stagnation point. Note that no combustion is assumed to take place when hydrogen is injected.

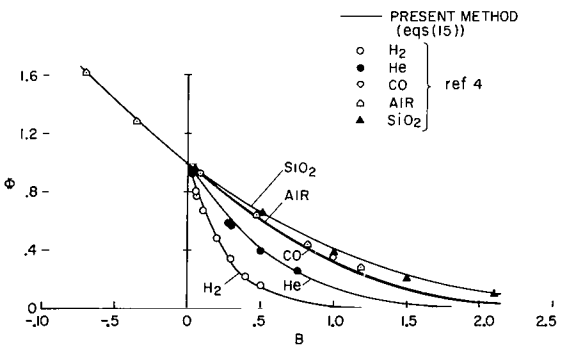

Figure 5.– Effect of foreign gas injection on shear reduction (p_s = 1 atm, $T_s \simeq$ 15,000° K, and $T_w/T_s \simeq 0$).

Effect of Postcooling on Shear Reduction

The effect of postcooling on the stagnation-point flow is (1) to reduce the driving enthalpy which changes the transport properties, and (2) to reduce the effective tangential velocity due to the shear stress in the shock layer, which lowers the shear stress at the body surface. As shown in reference 1, the enthalpy behind the shock wave varies with Stanton number and blowing rate. The present analysis gives a similar result for tangential velocity as shown in figure 6. The results were obtained from numerical solutions of equation (10) since the first-order solution neglects the postcooling effects.[4] The immediate effect of the shear stress on the velocity ratio behind the shock wave is noted. This is due to the nonzero value of the velocity gradient (eq. (11a)) and thus to the finite value of shearing stress ratio at the shock wave. Since the velocity (also enthalpy) varies with Stanton number and blowing rate, the shear reduction for air injection is altered in the manner shown in figure 7. For a small Stanton number the shear reduction is the same as obtained from the first-order solution (e.g., fig. 3). The shear reduction becomes less effective, however, as the Stanton number increases beyond the critical number, $(St)_{cr} \simeq 0.32$ (see ref. 1), and, finally, Φ approaches the free molecular limit of unity as $(St)_0 \to 1$. Similar results are shown in reference 1 for the heat reduction.

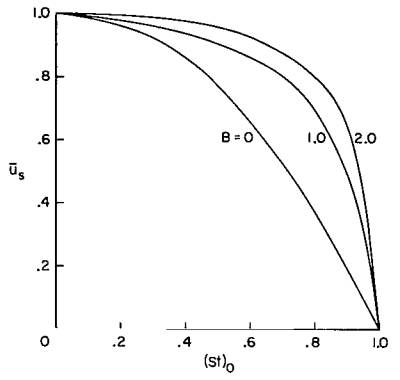

Figure 6.– Effect of Stanton number on tangential velocity behind shock wave – air injection (p_s = 1 atm, $T_s \simeq 15{,}000°$ K, and $T_w/T_s \simeq 0$).

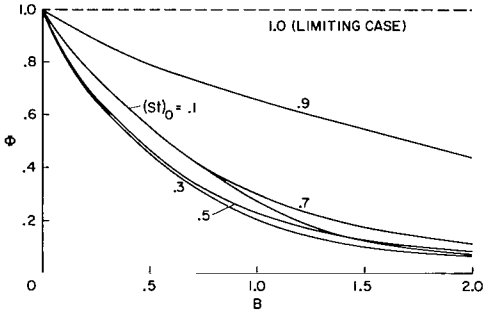

Figure 7.– Effect of Stanton number on shear reduction – air injection (p_s = 1 atm, $T_s \simeq 15{,}000°$ K, and $T_w/T_s \simeq 0$).

The critical Stanton number, at which the effect of postcooling becomes important, can be defined in terms of the physical parameters through the effective Peclet number β^* (see eq. (7c)). From figure 10(a) of reference 1, the effective Peclet number is found to be approximately $\beta^* \simeq 5$ for $(St)_{cr} \simeq 0.32$. Thus, one can show, in an actual flight case where $V_\infty \simeq 15$ km/sec, that the effect of postcooling on convective heat and shear stress becomes important when the product of the free-stream density and body radius becomes $\bar{\rho}_\infty R \lesssim 3\times10^{-4}$ cm, which corresponds to a flight altitude of 58 km for a body radius of $R \lesssim 1$ cm, or a flight altitude of 84 km for a body radius of $R = 30$ cm (1 ft).

---

[4]The computing program has been prepared by Mrs. Sarah Rogallo, NASA, Ames Research Center.

CONCLUDING REMARKS

Closed-form solutions have been obtained for the reduction of the shear gradient normal to the surface in the vicinity of the stagnation point of a body with mass transfer. The shock-layer momentum equation was decoupled from the continuity and energy equations by approximating the mass-flow distribution along the stagnation stream line. The momentum equation is then linearized by the introduction of an effective Reynolds number which is a constant for a given boundary temperature. The linearized solution indicates conclusions similar to those for the heat transfer for the reduction of the shear gradient at the stagnation point by mass addition, which represents the direct reduction of skin friction in the vicinity of the stagnation point.

1. The degree of reduction depends on the mass-addition rate and the Stanton number for no mass addition. For a given mass-addition rate, the shear-reduction rate increases with increasing Stanton number until the Stanton number reaches the critical value of about 0.32. The shear reduction becomes less effective as the Stanton number increases beyond the critical number and approaches the free molecule flow limit of unity.

2. The shear reduction depends on wall temperature; the higher the wall temperature, the less the reduction in shear stress.

3. The injection of gases of lower molecular weight is most effective for the shear reduction.

Ames Research Center
National Aeronautics and Space Administration
Moffett Field, Calif., 94035, June 11, 1970

APPENDIX A

TANGENTIAL MASS FLOW GRADIENT

The relation between the tangential and normal mass flow gradient in the vicinity of the stagnation point can be derived as follows:

The continuity equation (eq. (1)), with the effect of shock-layer thickness taken into account, is

$$\frac{\partial}{\partial x}(\rho u r) + \frac{\partial}{\partial y}(Q \rho v r) = 0$$

where $Q = 1 + y/R$ and $r = Qx$. If it is assumed that $\rho u \simeq [\partial(\rho u)/\partial x]x$ and $\rho v \simeq [\partial(\rho v)/\partial y]y$, the tangential mass-flow gradient and momentum become

$$\frac{\partial(\rho u)}{\partial x} \simeq -\left(\frac{3}{2} Q - 1\right) \frac{\partial(\rho v)}{\partial y} \tag{A1}$$

$$\rho u \left(\frac{\partial u}{\partial x}\right) \simeq \frac{1}{\rho_s} \left[\frac{\partial(\rho u)}{\partial x}\right]^2 x \tag{A2}$$

To allow for the velocity gradient at the shock wave, equation (A1) is modified as

$$\frac{\partial(\rho u)}{\partial x} = -c_r \left(\frac{3}{2} Q - 1\right) \frac{\rho_\infty V_\infty}{L} \left(\frac{\partial \chi}{\partial \eta}\right) \tag{A3}$$

where the factor c_r is determined from the boundary condition for the tangential mass-flow gradient at the shock wave,

$$\frac{\partial(\rho u)}{\partial x} = \bar{u}_s \left(\frac{\rho_s V_\infty}{R}\right) = \bar{u}_s \left(k_a \frac{\rho_\infty V_\infty}{L_o}\right) \tag{A4}$$

Thus, from equations (A3) and (A4), c_r is given by

$$c_r = -\frac{L}{L_o} \left(\frac{2k_a}{1 + 3 \frac{L}{L_o} k_a \varepsilon}\right) \frac{\bar{u}_s}{\chi_s'} \tag{A5}$$

For hypersonic flow where $\varepsilon << 1$ and $\chi_w << 1$ it follows, from equation (A3), that

$$\frac{\partial(\rho u)}{\partial x} = k_a \frac{\rho_\infty V_\infty}{L_o} \bar{u}_s \left(\frac{1 + 3k_a\varepsilon \frac{L}{L_o} \eta}{1 + 3k_a\varepsilon \frac{L}{L_o}} \right) \frac{\chi'}{\chi_s'} \simeq k_a \frac{\rho_\infty V_\infty}{L_o} \bar{u}_s \left(\frac{\chi'}{\chi_s'} \right) \tag{A6}$$

Thus, equation (A2) incorporating equation (A6) can now be written as

$$\frac{L}{\rho_\infty V_\infty U} \left(\rho u \frac{\partial u}{\partial x} \right) \simeq k_a \frac{L}{L_o} \left(\bar{u}_s \frac{\chi'}{\chi_s'} \right)^2 \tag{A7}$$

which is the result introduced in equation (7a).

APPENDIX B

THE EFFECTIVE THERMAL AND TRANSPORT PROPERTY PARAMETERS

Values for the effective Peclet number and Reynolds number which will be used in the linearized solution (eqs. (10) and (15)) are derived in this appendix.

THE EFFECTIVE PECLET NUMBER

Let δ_1 be defined as

$$q_{co}\delta_1 \equiv \int_o^L q \, dy \tag{B1}$$

where $q = [(k/c_p)(dh/dy)]$ and also $\delta^\dagger$ to be

$$\delta^\dagger \equiv \frac{\int_o^L (dh/dy)\,dy}{(dh/dy)_w} \tag{B2}$$

It follows, from equations (B1) and (B2), that

$$\left.\begin{aligned} q_{co} &= \left(\frac{k}{c_p}\right)^* \left(\frac{dh}{dy}\right)_w \left(\frac{\delta^\dagger}{\delta_1}\right) \\ \text{where} \quad \left(\frac{k}{c_p}\right)^* &= \frac{\int_o^L q \, dy}{\int_o^L (dh/dy)\,dy} = \frac{\int_o^{h_s} (k/c_p)\,dh}{\int_o^{h_s} dh} \qquad \text{for} \quad h_w = 0 \end{aligned}\right\} \tag{B3}$$

Note that the averaged value $(k/c_p)^*$ requires no knowledge of the solution. Now, assume that the variable (k/c_p) can be replaced by some appropriate constant value, say $(k/c_p) = X$; it then follows, from equations (B1), (B2), and (B3), that

$$\left.\begin{aligned} \frac{\delta^\dagger}{\delta_1} &= 1 \\ \text{and} \quad q_{co} &= X\left[\frac{dh}{dy}\,(X)\right]_w \end{aligned}\right\} \tag{B4}$$

When equation (B4) is compared with equation (B3), the most reasonable value of the effective constant X is,

$$X = \left(\frac{k}{c_p}\right)^*$$

and

$$q_{co} = \left(\frac{k}{c_p}\right)^* \left(\frac{dh}{dy}\right)_w^* \tag{B5}$$

The effective Peclet number is thus

$$\beta^* = \frac{\rho_\infty V_\infty L}{\left(\frac{k}{c_p}\right)^*} \tag{B6}$$

Table 1 presents some numerical calculations of the effective thermal and transport property parameter which are used in the first-order and general solutions. Table 1 seems to provide better results and has a more logical basis than that given in reference 1.

TABLE 1.– THERMAL TRANSPORT PROPERTIES, $(k/c_p)^*/(k/c_p)_{ref}$ [a]

P, atm / T, °K	10^2	10	1	10^{-1}	10^{-2}	10^{-3}	10^{-4}
0	0.0000000	0.0000000	0.0000000	0.0000000	0.0000000	0.0000000	0.0000000
1000	.6126295	.6126295	.6126295	.6126295	.6126295	.6126295	.6126295
2000	.9499233	.9502330	.9520912	.9559015	.9728052	1.0208307	1.1343960
3000	1.2197483	1.2552291	1.3579450	1.4889271	1.5654652	1.8207278	1.5203098
4000	1.5759500	1.7378318	1.8327561	1.7297006	1.7252176	1.9953843	1.9555636
5000	1.9541369	1.9647090	1.9875224	2.0680217	2.3124995	2.5002307	2.4097264
6000	2.1406367	2.2481930	2.4740788	2.6755975	2.6202073	2.4553741	2.4686934
7000	2.4545306	2.7457312	2.9321786	2.7763997	2.6461656	2.7342026	3.0686967
8000	2.9100277	3.1459877	3.0117004	2.8403820	3.0464870	3.6058875	4.6225201
9000	3.3108144	3.2662349	3.0849595	3.3162889	3.9997432	5.1343087	5.6699780
10000	3.5217905	3.3439494	3.4486317	4.2053297	5.4051008	6.0928483	5.7321583
11000	3.6278065	3.6939754	4.1170344	5.4612288	6.4812224	6.2490610	5.6746416
12000	3.7265962	4.2138305	5.0633505	6.6742440	6.8617359	6.2177217	5.6041260
13000	3.9544243	4.8933558	6.1638561	7.4202914	6.9172425	6.1587323	5.5313316
14000	4.4721040	5.7415978	7.1545277	7.7161356	6.8953037	6.0941142	5.4617239
15000	5.1004932	6.6690641	7.8287131	7.8154403	6.8470945	6.0360700	5.4029145

[a] $k/c_p = \mu/Pr$; $(k/c_p)_{ref} = 36.9 \times 10^{-6}$ lbm/sec-ft or $= 550 \times 10^{-6}$ gm/sec-cm; $T_{ref} = 1{,}000°$ K.

THE EFFECTIVE REYNOLDS NUMBER

Accurate calculations of heat transfer to the surface can be obtained if the average Peclet number β^{**} is used for general wall temperatures in the energy equation. Similarly, the effective Reynolds number Re^{**} may be introduced into the momentum equation where Re^{**} is related to β^{**} by

$$\left.\begin{aligned} Re^{**} &= \frac{\beta^{**}}{(Pr)^{**}} \qquad \text{for } \frac{T_w}{T_s} \neq 0 \\ \text{where } (Pr)^{**} &\text{ is approximated by} \\ (Pr)^{**} &= (Pr)_w^n \end{aligned}\right\} \tag{B7}$$

For $T_w/T_s \simeq 1$, $(Pr)^{**}$ becomes the Prandtl number for the wall temperature, and $n = 1$. For $T_w/T_s \simeq 0$ the results of reference 2 (ch. 4) yields $Re^* \simeq \beta^*/(Pr)_w^{2/3}$, and it can be shown that $(Pr)_w^{2/3} \simeq (Pr)_w$ since the Prandtl number is near unity for the lower wall temperature. Thus, the effective Reynolds number covering the intermediate wall temperature case is approximated simply by

$$(Re)^{**} \simeq \frac{\beta^{**}}{(Pr)_w} \tag{B8}$$

APPENDIX C

EQUATIONS FOR THE PHYSICAL PARAMETERS

BOUNDARY-LAYER THICKNESS

An important physical dimension in the viscous layer is the characteristic thickness $\delta^\dagger$, arbitrarily defined in equation (B2) as

$$\left(\frac{\delta^\dagger}{L}\right) \equiv \frac{\int_0^1 (d\bar{h}/d\eta)\,d\eta}{(d\bar{h}/d\eta)_w}$$

Since from reference 1,

$$\left(\frac{d\bar{h}}{d\eta}\right)_w = \sqrt{\frac{2}{\pi}(\beta_o \chi_w')^*}\,\frac{L}{L_o}\,\psi$$

it follows that

$$\left(\frac{\delta^\dagger}{L}\right) = \frac{1}{\sqrt{\frac{2}{\pi}(\beta_o \chi_w')^*}}\,\frac{L_o/L}{\psi} \qquad \text{for } \bar{h}_w \simeq 0 \cdot \tag{C1}$$

The thermal boundary-layer thickness for $\chi_w = 0$ is from reference 1,

$$\left(\frac{\delta}{L}\right)_o = \frac{1.8}{\sqrt{\frac{1}{2}(\beta_o \chi_w')^*}} \simeq 2\left(\frac{\delta^\dagger}{L}\right)_o \tag{C2}$$

Thus,

$$\left(\frac{\delta}{L}\right)_o \simeq \sqrt{\frac{2\pi}{(\beta_o \chi_w')^*}} = \frac{\pi (St)_o}{(\chi_w')^*} \tag{C3}$$

Similarly, the characteristic thickness corresponding to the momentum equation (from the homogeneous solution, eq. (12)) may be written as

$$\left(\frac{\delta_u{}^\dagger}{L}\right)_o = \frac{1}{\sqrt{\frac{2}{\pi}(Re_o \chi_w')^*}} = \sqrt{(Pr)_w}\left(\frac{\delta^\dagger}{L}\right)_o \tag{C4}$$

The velocity boundary-layer thickness is, thus

$$\left(\frac{\delta_u}{L}\right)_o \simeq 2\left(\frac{\delta_u{}^\dagger}{L}\right)_o = \sqrt{(Pr)_w}\ \left(\frac{\delta}{L}\right)_o = \sqrt{\frac{2\pi}{(Re_o \chi_w')^*}} \tag{C5}$$

BASIC FLOW PARAMETERS

The approximate relations for the basic flow parameters taken from reference 1 are:

Mass-flow gradient for $T_w/T_s \simeq 0$:

$$(\chi_w')^* \simeq k_a \sqrt{8\varepsilon(1 - \varepsilon)} \tag{C6}$$

(see eq. (7c) for k_a).

Mass-flow gradient for $T_w/T_s \neq 0$:

$$(\chi_w')^{**} \simeq k_w(\chi_w')^* \tag{C7}$$

where the factor $k_w = (k/c_p)^*/(k/c_p)^{**}$ depends on wall temperature (ref. 1).

Shock-layer thickness:

$$\frac{L}{L_o} = 1 + k_b\sqrt{\frac{1}{\varepsilon}\left(\frac{M_\infty}{M_f}\right)}\,\chi_w$$

or, from equation (13),

$$\frac{L}{L_o} = 1 + k_b\sqrt{\frac{1}{\varepsilon}\left(\frac{M_\infty}{M_f}\right)}\,(St)_o B \tag{C8}$$

where k_b depends on the body shape ($k_b = 1.0$ for an axisymmetric body).

The effective blowing parameter for the boundary-layer blowoff:

Blowoff is the situation where the increase in the shock-layer thickness is equal to the original boundary-layer thickness. From equations (C3) and (C8),

$$B_* = \frac{\pi\sqrt{\varepsilon\,(M_f/M_\infty)}}{(\chi_w')^*} \tag{C9}$$

Similarly, from equation (C5)

$$B_{\dagger} = \frac{\pi\sqrt{(Pr)_w \varepsilon (M_f/M_\infty)}}{(\chi_w')^*} = \sqrt{(Pr)_w}\, B_* \qquad (C10)$$

Equation (C10) is given in equation (15c).

APPENDIX D

FIRST-ORDER SOLUTION TO THE MOMENTUM EQUATION

A closed form solution to the linearized equation (7a) is given by equation (10a). An explicit closed form solution, is obtained by taking only the leading term from the linearized solution. The shear reduction function Φ can be written, from equations (13), as

$$\Phi = \left\{ \frac{\left[\frac{(\overline{u}_c'/\mathrm{Re})^*_{w,B}}{(\overline{u}_c'/\mathrm{Re})^*_{w,B=0}} \right] + \left(\frac{1 - c_1}{c_1} \right) \frac{1}{\mathrm{Re}_{w,B}} \left(\frac{1}{\overline{u}_c'/\mathrm{Re}} \right)^*_{w,B=0}}{1 + \left(\frac{1 - c_1}{c_1} \right) \frac{1}{\mathrm{Re}_{w,B=0}} \left(\frac{1}{\overline{u}_c'/\mathrm{Re}} \right)^*_{w,B=0}} \right\} \tag{D1}$$

The first term in the numerator of equation (D1) takes exactly the same form as the heat reduction function except that the blowing parameter B is replaced by $B/\sqrt{(\mathrm{Pr})_w}$,

$$\frac{(\overline{u}_c'/\mathrm{Re})^*_{w,B}}{(\overline{u}_c'/\mathrm{Re})^*_{w,B=0}} = \frac{(\overline{h}'/\beta)^*_{w,B/\sqrt{(\mathrm{Pr})_w}}}{(\overline{h}'/\beta)^*_{w,B=0}}$$

$$= \phi(\lambda, B/\sqrt{(\mathrm{Pr})_w}) \tag{D2}$$

where ϕ is given in equation (15b) taken from reference 1. The second term in the numerator may be rearranged as

$$\frac{(1 - c_1)}{c_1} \frac{1}{(\mathrm{Re})_{w,B}} \left(\frac{1}{\overline{u}_c'/\mathrm{Re}} \right)^*_{w,B=0} = \frac{(1 - c_1)}{2c_1} \frac{\mathrm{Re}_o^*}{\mathrm{Re}^*} \frac{\mathrm{Re}^*}{(\mathrm{Re})_{w,B}} \sqrt{\frac{2\pi}{(\mathrm{Re}_o \chi_w')^*}} \tag{D3}$$

Since $\mathrm{Re}^* = \beta^*/(\mathrm{Pr})_w$ and $(\overline{u}_c')_{w,B=0} = \sqrt{(2/\pi)(\mathrm{Re}_o \chi_w')^*}$, and from equation (C5), it follows that

$$\frac{(1 - c_1)}{c_1 (\mathrm{Re})_{w,B}} \left(\frac{1}{\overline{u}_c'/\mathrm{Re}} \right)^*_{w,B=0} = \frac{(1 - c_1)}{2c_1} \left(\frac{\delta_u}{L} \right)_o \frac{(k/c_p)_w}{(k/c_p)^*} \left(\frac{L_o}{L} \right) \tag{D4}$$

The characteristic thicknesses of the present solution (eqs. (B2) and (C5)) and the proper boundary conditions require that equation (D1) should be evaluated for the condition

$$\left(\frac{\delta_u}{L}\right)_o \simeq 1 \tag{D5}$$

since the characteristic length determined from the velocity distribution, for $u/u_s \simeq 0.99$, is always the same as the shock-layer thickness.

A general form of equation (D1) incorporating equations (D2) through (D5), thus, becomes

$$\Phi = \left\{ \frac{\phi\left[\lambda, \dfrac{B}{\sqrt{(Pr)_w}}\right] + \gamma \dfrac{(k/c_p)_w}{(k/c_p)^*} \dfrac{L_o}{L}}{1 + \gamma \dfrac{(k/c_p)_w}{(k/c_p)^*}} \right\} \tag{D6}$$

In hypersonic flows where $\varepsilon << 1$, the factor γ is close to unity.

For $T_w/T_s \simeq 0$, only the first term in equation (D6) need be retained, thus,

$$\Phi \simeq \phi\left[\lambda, \frac{B}{\sqrt{(Pr)_w}}\right] \tag{D7}$$

The result, exactly analogous to equation (D6), can be derived for the cases where $T_w/T_s \neq 0$; that is, from equations (B8) and (C7), equation (D3) can be written

$$\frac{(1 - c_1)}{c_1 (Re)_{w,B}} \left(\frac{1}{\overline{u}_c'/Re}\right)^{**}_{w,B=0} = \frac{(1 - c_1)}{2c_1} \frac{Re_o^{**}}{Re^{**}} \frac{Re^{**}}{(Re)_{w,B}} \sqrt{\frac{2\pi}{(Re_o \chi_w')^{**}}}$$

$$= \frac{(1 - c_1)}{2c_1} \frac{L_o}{L} \left(k_w \frac{\beta^*}{\beta_w}\right) \frac{1}{k_w} \left(\frac{\delta_u}{L}\right)_o \tag{D8}$$

which is the same as equation (D4). Equation (D6) which is the result shown in equations (15), therefore, is applicable for all wall temperature.

REFERENCES

1. Yoshikawa, Kenneth K.: Linearized Theory of Stagnation Point Heat and Mass Transfer at Hypersonic Speeds. NASA TN D-5246, 1969.

2. Dorrance, W. H.: Viscous Hypersonic Flow. McGraw-Hill Book Co., 1962.

3. Howe, John T.; and Sheaffer, Yvonne S.: Mass Addition in the Stagnation Region for Velocity up to 50,000 Feet Per Second. NASA TR R-207, 1964.

4. Anfimov, N. A.; and Al'tov, V. V.: Heat Transfer, Friction, and Mass Transfer in a Laminar Multicomponent Boundary Layer with Injection of a Foreign Gas. International Chemical Engineering, vol. 6, no. 1, Jan. 1966, pp. 137-144.

5. Pappas, C. C.; and Lee, G.: Effects of Mass Addition of Various Gases on the Heat Transfer and Surface Pressures on a Blunt Cone in Hypersonic Flow. AIAA paper 69-716, AIAA Fluid and Plasma Dynamics Conference, San Francisco, June 16-18, 1969.

6. Chen, S. Y.; Baron, J.; and Mobley, R.: Stagnation Region Gas Injection in Low Reynolds Number Hypersonic Flow. Proc. 1967 Heat Transfer and Fluid Mechanics Inst., Paul A. Libby, Daniel B. Olfe, and Charles W. Van Atta, eds., Stanford, Calif., Stanford Univ. Press, 1967, pp. 34-57.

7. Yoshikawa, Kenneth K.: A Simplified Solution of Stagnation Point Heat, Shear Stress, and Mass Transfer at Hypersonic Speeds. Paper presented at the 6th U. S. National Congress of Applied Mechanics, Harvard Univ., Cambridge, Mass., June 15-19, 1970.

NASA-Langley, 1971 — 12 A-3677

"The aeronautical and space activities of the United States shall be conducted so as to contribute . . . to the expansion of human knowledge of phenomena in the atmosphere and space. The Administration shall provide for the widest practicable and appropriate dissemination of information concerning its activities and the results thereof."

— NATIONAL AERONAUTICS AND SPACE ACT OF 1958

NASA SCIENTIFIC AND TECHNICAL PUBLICATIONS

TECHNICAL REPORTS: Scientific and technical information considered important, complete, and a lasting contribution to existing knowledge.

TECHNICAL NOTES: Information less broad in scope but nevertheless of importance as a contribution to existing knowledge.

TECHNICAL MEMORANDUMS: Information receiving limited distribution because of preliminary data, security classification, or other reasons.

CONTRACTOR REPORTS: Scientific and technical information generated under a NASA contract or grant and considered an important contribution to existing knowledge.

TECHNICAL TRANSLATIONS: Information published in a foreign language considered to merit NASA distribution in English.

SPECIAL PUBLICATIONS: Information derived from or of value to NASA activities. Publications include conference proceedings, monographs, data compilations, handbooks, sourcebooks, and special bibliographies.

TECHNOLOGY UTILIZATION PUBLICATIONS: Information on technology used by NASA that may be of particular interest in commercial and other non-aerospace applications. Publications include Tech Briefs, Technology Utilization Reports and Technology Surveys.

Details on the availability of these publications may be obtained from:

SCIENTIFIC AND TECHNICAL INFORMATION OFFICE

NATIONAL AERONAUTICS AND SPACE ADMINISTRATION

Washington, D.C. 20546